AGU PUBLICATIONS

Geophysical Research Letters

RESEARCH LETTER
10.1002/2017GL073862

Key Points:
- Models forced with identical ozone depletion can yield different lower stratospheric cooling
- The difference is due to a dynamical feedback dependent on the polar vortex climatology
- Biases in the polar vortex climatology may lead to incorrect response to ozone depletion

Supporting Information:
- Supporting Information S1

Correspondence to:
P. Lin,
pulin@princeton.edu

Citation:
Lin, P., D. Paynter, L. Polvani, G. J. P. Correa, Y. Ming, and V. Ramaswamy (2017), Dependence of model-simulated response to ozone depletion on stratospheric polar vortex climatology, *Geophys. Res. Lett.*, *44*, 6391–6398, doi:10.1002/2017GL073862.

Received 17 APR 2017
Accepted 8 JUN 2017
Accepted article online 12 JUN 2017
Published online 28 JUN 2017

Dependence of model-simulated response to ozone depletion on stratospheric polar vortex climatology

Pu Lin[1], David Paynter[2], Lorenzo Polvani[3,4], Gustavo J. P. Correa[4], Yi Ming[2], and V. Ramaswamy[2]

[1]Program in Atmospheric and Oceanic Sciences, Princeton University, Princeton, New Jersey, USA, [2]Geophysical Fluid Dynamics Laboratory/NOAA, Princeton, New Jersey, USA, [3]Department of Applied Physics and Applied Mathematics, Columbia University, New York, New York, USA, [4]Lamont-Doherty Earth Observatory, Palisades, New York, USA

Abstract We contrast the responses to ozone depletion in two climate models: Community Atmospheric Model version 3 (CAM3) and Geophysical Fuild Dynamics Laboratory (GFDL) AM3. Although both models are forced with identical ozone concentration changes, the stratospheric cooling simulated in CAM3 is 30% stronger than in AM3 in annual mean, and twice as strong in December. We find that this difference originates from the dynamical response to ozone depletion, and its strength can be linked to the timing of the climatological springtime polar vortex breakdown. This mechanism is further supported by a variant of the AM3 simulation in which the southern stratospheric zonal wind climatology is nudged to be CAM3-like. Given that the delayed breakdown of the southern polar vortex is a common bias among many climate models, previous model-based assessments of the forced responses to ozone depletion may have been somewhat overestimated.

1. Introduction

Stratospheric ozone over Antarctica has undergone severe reduction over the past few decades [*Solomon*, 1999, and references therein]. This atmospheric composition change alters the atmospheric radiative balance and cools the stratosphere [*Shine*, 1987; *Ramaswamy et al.*, 1992; *Forster and Shine*, 1997], with the southern annular mode shifting to its positive polarity [*Thompson and Solomon*, 2002]. The most prominent feature of this anomalous circulation pattern is the poleward shift of the extratropical jet in the troposphere during austral summer [e.g., *Son et al.*, 2010; *Polvani et al.*, 2011]. The poleward shift of the jet may further induce changes in the tropical Hadley circulation [*Polvani et al.*, 2011], precipitation [*Kang et al.*, 2011], cloudiness [*Grise et al.*, 2013], and ocean ventilation [*Waugh et al.*, 2013]. Many studies attributed most of the circulation changes in the Southern Hemisphere over recent decades to ozone depletion [e.g., *Arblaster and Meehl*, 2006; *Son et al.*, 2010; *Polvani et al.*, 2011; *McLandress et al.*, 2011; *Lee and Feldstein*, 2013].

The circulation response to ozone depletion has been simulated by many global climate models (GCMs) both with prescribed and interactively driven ozone losses [e.g., *Ramaswamy et al.*, 2001; *Arblaster and Meehl*, 2006; *Son et al.*, 2010; *Polvani et al.*, 2011; *McLandress et al.*, 2011; *Gerber and Son*, 2014]. Although almost all models simulate the lower stratospheric cooling and the poleward shift of the jet in response to ozone depletion, the magnitude differs vastly among models. For Coupled Model Intercomparison Project Phase 5 (CMIP5) models, the simulated cooling trend over the historical period varies by a factor of 2, and the associated jet shift ranges from near zero to over 0.5° per decade [*Gerber and Son*, 2014]. Models with interactive stratospheric chemistry show even greater spread [*Butchart et al.*, 2010; *Gerber and Son*, 2014].

Efforts have been made to reconcile the divergent responses to ozone depletion simulated by climate models. Part of the discrepancy is ascribed to differences in stratospheric ozone change itself and large internal variability [*Waugh et al.*, 2015]. By analyzing a hierarchy of climate model simulations, *Seviour et al.* [2017] reported a consistent extratropical jet shift being proportional to the lower stratospheric cooling. In this paper, we ask a yet simpler question: does prescribing identical ozone forcing yield identical lower stratospheric cooling across different models? The answer happens to be no. We demonstrate this by analyzing model output from long "time-slice" integrations of two different models forced with identical stratospheric ozone changes. We use time-slice integrations to cleanly extract the forced response from the internal variability. Exploring the cause of the different cooling response caused by identical ozone changes, we show that it is related to

different biases in the climatological stratospheric circulation in the models, notably the timing when the polar stratospheric winds transition from westerly to easterly in the late spring.

2. Model Description

The first model employed in this study is the Community Atmospheric Model version 3 (CAM3) [*Collins et al.*, 2006]. It is run at T42 horizontal resolution (~2.8° × 2.8°) with 26 hybrid vertical levels. Eight of the model levels are located above 100 hPa and the model top is at 2.2 hPa. The simulations analyzed here are extensions of those in *Polvani et al.* [2011]. The model specifies ozone concentrations, sea surface temperatures (SSTs), and sea ice concentrations (SICs) as repeating seasonal cycles. Other external forcings such as greenhouse gases and insolation are held constant. We contrast a pair of "time-slice" simulations in which ozone concentrations are specified as in year 1960 or 2000 with all other forcings being held at the 2000 levels (viz. GHG2000 and BOTH2000 in *Polvani et al.* [2011]). They are referred to as 1960ozone and 2000ozone, respectively. Year 1960 is chosen as a representative year before the formation of Antarctic ozone hole, and year 2000 reflects an ozone-depleted condition. The ozone data set is from *Cionni et al.* [2011] (recommended for CMIP5 simulations). Each simulations spans 100 model years, the last 60 of which are analyzed.

Similar simulations are conducted with the Geophysical Fuild Dynamics Laboratory (GFDL) AM3 [*Donner et al.*, 2011]. This model has a horizontal resolution of ~200 km and 48 vertical levels. Twenty-five model levels are above 100 hPa with a model top at 0.01 hPa. The standard AM3 equipped with fully interactive stratospheric chemistry is capable of prognosticating stratospheric ozone concentrations. Here for a clean comparison with CAM3, we choose to drive AM3 with the same prescribed ozone concentrations. SSTs, SICs, and all other external forcings are held at year 2000 levels in AM3. All AM3 simulations last 61 model years, with the first year as spin-up. We also performed simulations with a version of GFDL AM4 that has a low model top (1 hPa) and low vertical resolution in the stratosphere (9 model levels above 100 hPa), and the results are similar to those with AM3 (not shown).

An additional pair of simulations is conducted using AM3, in which the stratospheric zonal wind climatology in the Southern Hemisphere is forced to be CAM3-like. This is done by applying an artificial tendency to zonal mean zonal wind in the region poleward of 20°S and above 200 hPa. All other settings are the same as the original AM3 simulations. We denoted these simulations as AM3C. More details of AM3C are given in the Appendix.

Finally, we note that in this paper the "response" associated with ozone depletion is calculated as the difference between the integrations with and without ozone hole (2000ozone minus 1960ozone), averaged over 60 years.

3. Results

We start by examining the monthly mean difference between the 2000ozone and the 1960ozone simulations in polar cap (averaged poleward of 60°S) temperature simulated with the two models. As shown in Figures 1a and 1b, both models simulate stratospheric cooling in response to ozone depletion. The cooling peaks at late spring/early summer and extends from middle to lower stratosphere over the course of a few months, a pattern that is also seen in observations [*Thompson and Solomon*, 2002]. The duration of the cooling is shorter in AM3 than in CAM3. There is no discernible difference in austral spring when the ozone-induced cooling first starts to develop. By summer, however, the cooling in CAM3 is almost twice as large as in AM3. The largest difference, over 6 K, is found at ~70 hPa in December. In the lowermost stratosphere, the cooling begins to level off from February in AM3 but persists into March in CAM3. Consistent with the polar cap cooling, CAM3 also shows greater strengthening of the polar vortex from December to February.

Figure 2 shows the changes in the 100 hPa polar cap temperature, an often used index of stratospheric response to ozone depletion [e.g., *Gerber and Son*, 2014; *Seviour et al.*, 2017]. As shown in Figure 2, CAM3 and AM3 diverge significantly from December to April and overlap with each other for the rest of the year. The annual mean cooling at 100 hPa in CAM3 is about 30% larger than that in AM3, and the November–January (NDJ) mean is approximately 40% larger.

The stratospheric cooling associated with ozone depletion has its root cause in the reduced radiative heating by ozone [e.g., *Kiehl et al.*, 1988; *Mahlman et al.*, 1994; *Randel and Wu*, 1999]. The differing stratospheric cooling simulated by the two models, however, does not arise from notable difference in the initial radiative

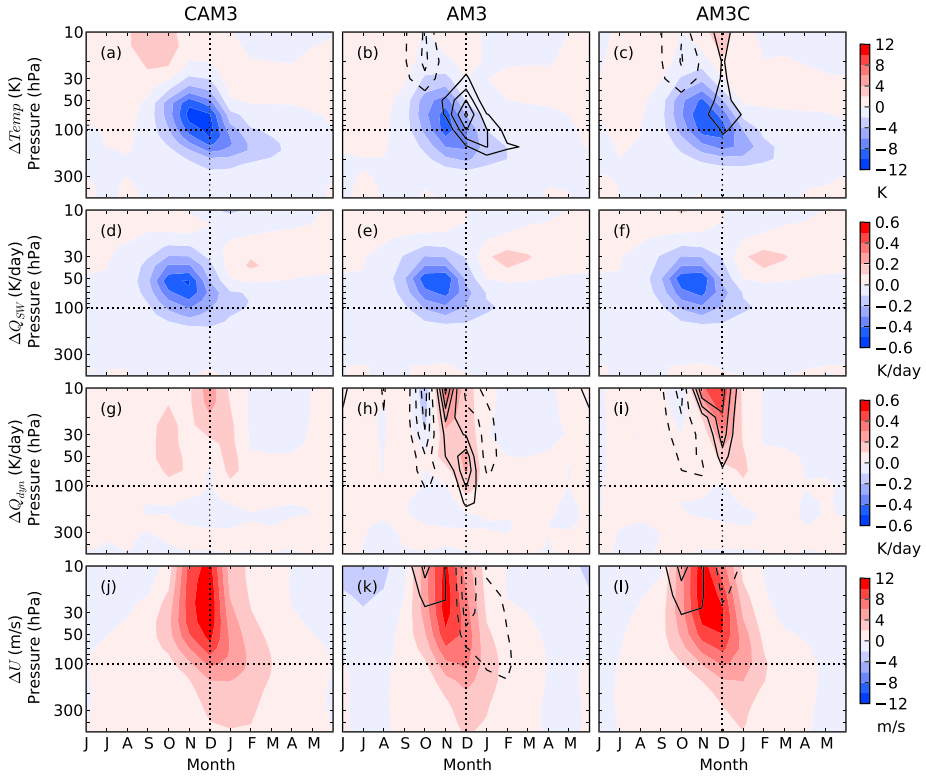

Figure 1. Responses to ozone depletion (2000ozone minus 1960ozone) in the monthly mean polar cap (a–c) air temperature, (d–f) shortwave heating rate, (g–i) dynamical heating rate, and (j–l) zonal mean zonal wind averaged over 50°S–70°S for CAM3 (Figures 1a, 1d, 1g, and 1j), AM3 (Figures 1b, 1e, 1h, and 1k), and AM3C (Figures 1c, 1f, 1i, and 1l). Black countours are for the differences relative to CAM3 (middle: AM3 minus CAM3; right: AM3C minus CAM3). Positive (negative) values are in solid (dashed) contours, with zero contour omitted. The countour interval is 1.5 K for temperature, 0.075 K day^{-1} for heating rates, and 2 m s^{-1} for zonal wind.

perturbation. As shown in Figures 1d and 1e, the shortwave heating rate changes due to ozone depletion are essentially identical. The radiative effect of ozone depletion also consists of a longwave component [*Kiehl and Boville*, 1988; *Ramasway and Bowen*, 1994], but it confounds with the longwave heating rates changes due to temperature changes and cannot be directly diagnosed. It is the difference in dynamical responses that sets apart the two models. Figure 1g indicates that CAM3 simulates an increase of the dynamical heating rate, which initiates at ~10 hPa in November and reaches the lower stratosphere by January. The pattern in AM3 is generally similar, except that the heating occurs about 1 month earlier than in CAM3. In November and December, the ozone-induced dynamical heating in AM3 exceeds that in CAM3 by as much as 0.2 K day^{-1}. This explains the substantially weaker stratospheric cooling in AM3 (up to 6 K).

The stratospheric circulation is dominated by the so-called Brewer-Dobson circulation, which has an ascending branch over the equator and descending branches in the extratropics [*Holton et al.*, 1995]. The descending motion leads to a dynamical warming in the polar stratosphere. The Brewer-Dobson circulation is driven by wave breaking, and wave propagation and dissipation are modulated by the background zonal wind structure in a complex fashion. According to linear theory, planetary waves originating in the troposphere can propagate vertically into the stratosphere only in westerlies. Stronger westerlies favor greater wave activity penetration into the stratosphere, and hence a more vigorous stratospheric circulation [*Charney and Drazin*, 1961].

This wave-mean flow interaction suggests a negative feedback in determining the thermal response to ozone depletion. A radiatively induced initial cooling of the polar cap causes a strengthening of the climatological westerly via the thermal wind relation, which in return facilitates wave propagation and gives rise to a stronger Brewer-Dobson circulation. The resulting enhancement of the dynamical heating over the polar cap has a tendency to offset part of the initial cooling. This dynamical response to ozone depletion has been reported

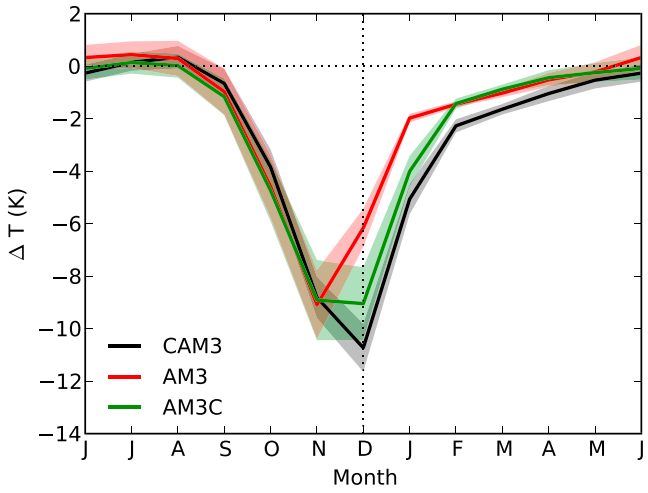

Figure 2. Difference in the polar cap temperature at 100 hPa between the 2000ozone and 1960ozone simulations. Shading indicates the 95% confidence interval based on the Student's *t* test.

in previous model studies [*Mahlman et al.*, 1994; *Manzini et al.*, 2003; *Li et al.*, 2008; *McLandress et al.*, 2010; *Lin and Fu*, 2013]. It has also been confirmed in the recent observational study by *Ivy et al.* [2016].

This negative feedback occurs only when the zonal wind is relatively weak that is when the polar vortex starts to break down. Wave propagation does not vary much with the polar vortex strength when it is already strong. To the contrary, an exceedingly strong polar vortex may even prohibit wave propagation, thus leading to a positive feedback on polar cap temperature. This explains why the ozone-depletion-induced dynamical heating is confined to late spring/early summer, when the polar vortex starts to break down, in our models as well as in other models reported in previous studies [*Manzini et al.*, 2003; *Li et al.*, 2008; *McLandress et al.*, 2010; *Lin and Fu*, 2013].

This dynamical mechanism would affect external forced changes and internal variations alike. We examine the latter in the 2000ozone simulations. Figure 3 shows the correlation between the interannual anomalies in dynamical heating rates at each level and the 50 hPa temperature in the previous month, overlaid with climatological zonal wind averaged over 50°S to 70°S. Both CAM3 and AM3 show a patch of strong negative correlation that is colocated with weak zonal winds (approximately less than 20 m s^{-1}), which occur mainly in NDJ. Similar correlation is also computed using the ERA interim reanalysis data (ERAi) [*Dee et al.*, 2011]. Dynamical heating rate is not a standard output variable for ERAi, and we calculated it as $-N^2Hw^*/R$, in which N is the buoyancy frequency, H is the scale height, w^* is the vertical velocity of the Brewer-Dobson circulation, and R is the air gas constant. As shown in Figure 3d, reanalysis data confirm such negative dynamical feedback. Note that this negative feedback would be masked in the concurrent correlation between dynamical heating rates and temperature as heating rates drive temperature changes resulting in a positive correlation. We find that the negative feedback is best shown when temperature leads dynamical heating rates by 1 month (based on monthly data).

Comparing Figures 1g and 1h versus Figures 3a and 3b, we see that the dynamical warming in response to ozone depletion is located where the negative correlations occur. This confirms that it is the same zonal wind climatology that determines the dynamical response to both ozone forcing and unforced interannual variations.

A closer inspection reveals that the polar vortex breakdown occurs in CAM3 at a later time than in AM3 or ERAi reanalysis (Figure 3). So does the negative dynamical feedback. In December when the two models exhibit the largest difference, the strong negative dynamical feedback already kicks in and dampens the radiative cooling in AM3, but not yet in CAM3. In fact, a slightly positive feedback in the lower stratosphere acts to enhance the radiative cooling in CAM3 at this time of the year. This difference in the timing of the negative dynamical feedback between the two models appears to be responsible for their divergent thermal responses to the same ozone forcing. This conclusion is consistent with the fact that during austral spring when the negative feedback is absent, the two models do agree with each other.

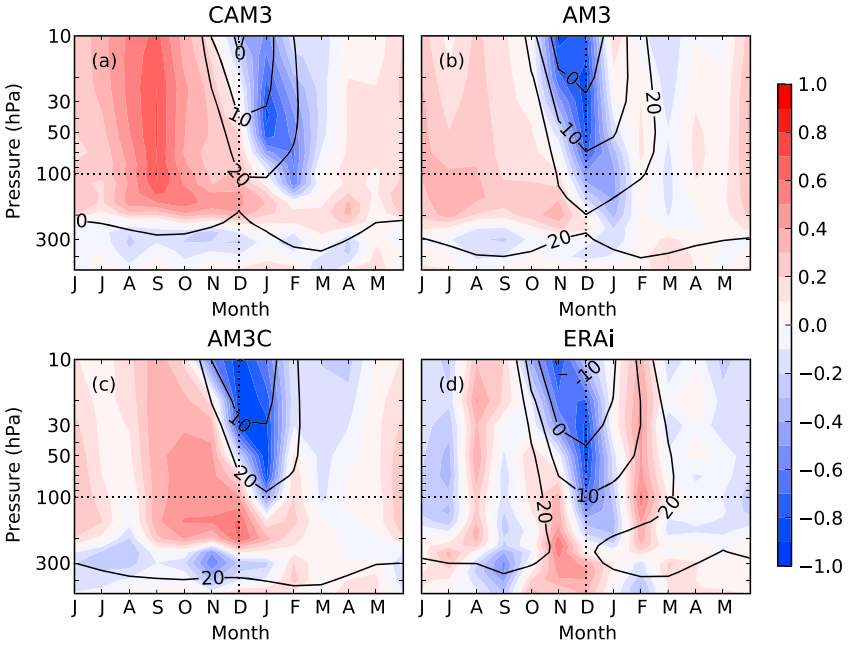

Figure 3. Correlation between the interannual anomalies in dynamical heating rates at each level and the 50 hPa temperature in the previous month (color shading), and the corresponding zonal wind averaged over 50°S–70°S (black contours) in the 2000ozone simulations of (a) CAM3, (b) AM3, and (c) AM3C. Both temperature and dynamical heating rates are averaged over the polar cap. For clarity, zonal winds stronger than 20 m s^{-1} are not shown. (d) As in Figure 3a except for ERA interim reanalysis for 1979–2014.

Note that the stratospheric cooling from ozone depletion itself will lead to a delay in the breakdown of the polar vortex [*Sun et al.*, 2014]. However, the delay in response to ozone depletion is minor compared to the difference in polar vortex climatology between the two models. This argument is supported by the fact that later polar vortex breakdown and later negative dynamical feedback in CAM3 than AM3 is also seen in the 1960ozone simulations (Figure S1 in the supporting information). The delayed polar vortex breakdown in CAM3 is consistent with its colder pole cap in spring (Figure S2).

To further confirm the role of climatological zonal wind in modulating the ozone-forced response, we conduct an additional pair of simulations called AM3C. In these simulations, we forced the simulated zonal mean zonal wind to have a similar seasonal cycle to that in CAM3. Figure 4 shows the zonal wind profiles for NDJ, the season when the polar vortex starts to break down and westerlies transit into easterlies from the upper stratosphere to lower stratosphere. It is clear that CAM3 simulates much stronger westerlies than AM3 or ERAi throughout the stratosphere for all 3 months. AM3C, on the other hand, produces similar zonal wind profile to CAM3. The 1960ozone simulations yield similar zonal wind profiles (Figure S3).

We repeat the above analysis for the AM3C simulations. With the perturbed zonal wind seasonal cycle, the negative dynamical feedback occurs in AM3C about 1 month later than AM3 (Figures 3c versus 3b) and so is the ozone-induced increase of dynamical heating (Figures 1i versus 1h). In terms of the magnitude of the stratospheric cooling, the perturbation in zonal wind seasonality also brings about a closer agreement with CAM3 than the original AM3 (Figures 1c versus 1b and Figure 2). The similarity between CAM3 and AM3C also indicates that any difference in longwave radiation schemes between the two models has minor effects here; otherwise, AM3C should behave like AM3 as they employed the same radiation scheme.

Previous studies have shown that the effect of ozone depletion is not limited to the polar stratosphere but is also manifested in the tropospheric circulation, notably in the location of the extratropical jet and the extent of Hadley cell [e.g., *Thompson and Solomon*, 2002; *Polvani et al.*, 2011; *Gerber and Son*, 2014]. Therefore, we now examine the ozone-induced response in the midlatitude jet, in terms of latitudinal shift of the maximum zonal mean zonal wind at 850 hPa. We find that the January–February mean poleward shift is 1.2°±0.5° in CAM3, 0.9°± 0.4° in AM3, and 1.2°± 0.4° in AM3C (uncertainty range is calculated based on the Student's *t* test at 95% confidence level). The key point is that the simulations with larger stratospheric cooling (CAM3 and AM3C)

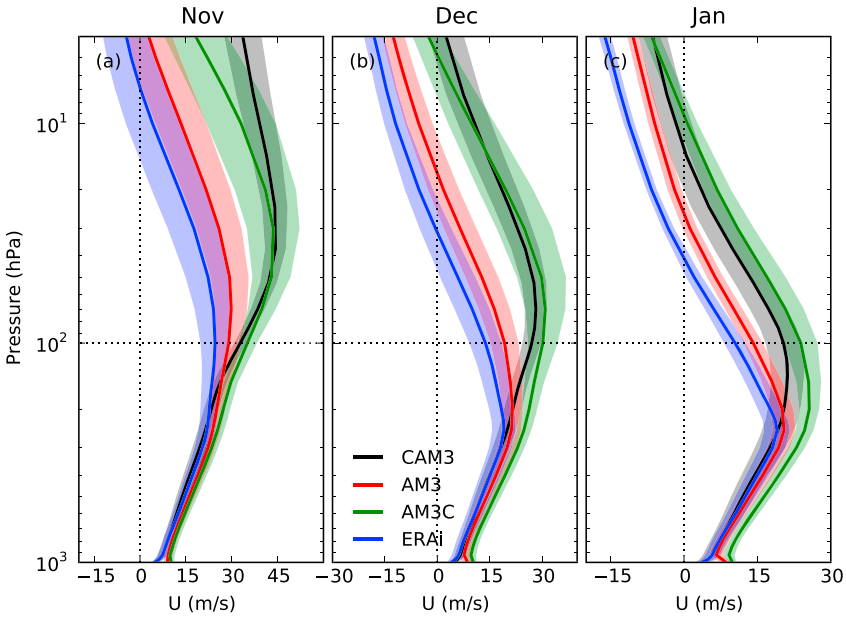

Figure 4. Profiles of zonal wind averaged over 50°S–70°S from the 2000ozone simulations for CAM3, AM3, and AM3C, and from 1979 to 2014 mean from ERA interim reanalysis in (a) November, (b) December, and (c) January. Shading indicates the 95% confidence interval based on the Student's *t* test.

show a larger jet shift, although one should not fail to note that the internal variability is comparable to the intermodel difference itself, and the intermodel difference in jet shift is therefore not statistically significant at that level. Similar conclusion is reached when diagnosing response in midlatitude jet in terms of the leading mode in extratropical winds (Figure S4). This confirms the recent finding by *Seviour et al.* [2017].

4. Summary and Discussion

We have compared the stratospheric temperature response to identical ozone forcing in two GCMs and find that one (CAM3) simulates stronger and more persistent stratospheric cooling than the other (AM3). The difference amounts to about 30% in annual mean, and a factor of 2 in December. The stronger temperature response in CAM3 arises from its delayed dynamical responses to ozone depletion, which originates from its delayed breakdown of the polar vortex. This is because the wave-mean flow interaction generates a negative dynamical feedback which affects polar temperature variations under weak polar vortex conditions. The ozone's radiative effect emerges in spring: the earlier this negative dynamical feedback takes hold, the more effective it is in dampening the direct radiative effect, and the weaker the net response to ozone forcing is. Stronger stratospheric cooling leads to stronger tropospheric wind anomalies in the following months, and a larger poleward shift of the extratropical jet. We confirm this mechanism with a variant of AM3 in which the zonal wind climatology is altered by applying an artificial tendency.

The delayed breakdown of the Southern Hemisphere polar vortex is a common bias suffered by many Chemistry-Climate models, which have better representation of the stratosphere and ozone chemistry than regular GCMs [*Butchart et al.*, 2011]. The findings presented above suggest that the ozone-forced response may be overestimated in these models. Indeed, *Baldwin et al.* [2010] reported an unrealistically stratospheric cooling in these models, even though the simulated ozone depletion was in agreement with observations. However, such bias may not always be apparent when comparing model-simulated circulation trends with observations. This is not only due to the uncertainty arising from the observations, which can be large over the southern polar region [*Calvo et al.*, 2012; *Young et al.*, 2013]. It is also due to the internal variability of the climate system, which can compensate and mask model biases. Two recent studies have shown that the internal variability is likely to play an important role in the observed Southern Hemisphere trends over the recent decades [*Wang and Waugh*, 2012; *Garfinkel et al.*, 2015]. This helps to explain why the ensemble mean response tend to be weaker than in the observations [*Johanson and Fu*, 2009; *Son et al.*, 2010; *Garfinkel et al.*, 2015], despite the possible overestimate of the ozone-forced changes documented here.

Lastly, it is worth noting that the stratospheric dynamical response to ozone depletion also manifests itself in the tropics. As part of the Brewer-Dobson circulation, any descent and warming in the polar region must be accompanied by ascent and cooling in the tropics. Increased tropical ascent dilutes ozone concentration in the lower stratosphere, leading to further cooling. Two recent studies [*Fu et al.*, 2015; *Polvani et al.*, 2017] suggest that the tropical lower stratospheric cooling observed from 1979 to 1997 is mainly due to the Southern Hemisphere ozone depletion, as opposed to greenhouse gases increase and global warming. As a consequence, there is reason to believe that any bias in the stratospheric polar vortex climatology would also translate into a bias in the trends of temperature and ozone in the tropical lower stratosphere. Given this wide range of downstream effects, our findings highlight the importance of reducing model biases in the polar vortex climatology.

Appendix A: Artificial Zonal Wind Tendency in AM3C

To obtain the artificial zonal wind tendency needed for nudging the zonal wind seasonal cycle of AM3 toward CAM3, we follow the "bias correction" method introduced by *Kharin and Scinocca* [2012]. We first run a nudged AM3 simulation in which the zonal winds are relaxed toward the mean seasonal cycle from CAM3 with a relaxation time scale of 5 days. For fair comparison, all forcings in both AM3 and CAM3 (including ozone, GHGs, and SSTs) are set to year 2000 levels in this case. We saved the relaxation tendency from this nudged simulation and averaged over the last 10 years of the 31 year simulation to construct a seasonal cycle of zonal mean zonal wind tendency. The resulting field is a function of latitude, level, and month. We, however, find that the tendency constructed this way is not sufficient for significantly delaying the polar vortex breakdown in AM3, possibly due to the fact that we chose a relatively long relaxation time scale for the nudged simulation. We then amplify the tendency by a factor of 1.5 for September and January, 1.7 for October and December, and 2 for November. This tendency is then applied to both 2000ozone and 1960ozone simulations.

Since we intend to only alter the seasonality of the Southern Hemisphere polar vortex, the nudging and bias correction are limited to poleward of 20°S and above 200 hPa. The simulated changes in climatological zonal wind, however, are not limited to this region, which may also contribute to the different responses in AM3 and AM3C, especially in the troposphere.

Acknowledgments
We thank Darryn Waugh for his helpful comments on this manuscript. This report was prepared by Pu Lin under award NA14OAR4320106 from the National Oceanic and Atmospheric Administration, U.S. Department of Commerce. The statements, findings, conclusions, and recommendations are those of the author(s) and do not necessarily reflect the views of the National Oceanic and Atmospheric Administration, or the U.S. Department of Commerce. L.M.P is funded by a grant from the U.S. National Science Foundation to Columbia University. The simulations used in the paper are permanently stored at the GFDL archive and are fully backed up. They are available upon request.

References

Arblaster, J. M., and G. A. Meehl (2006), Contributions of external forcings to Southern Annular Mode trends, *J. Clim.*, *19*, 2896–2905, doi:10.1175/JCLI3774.1.

Baldwin, M. P., et al. (2010), Effects of the stratosphere on the troposphere, in *SPARC Report on the Evaluation of Chemistry-Climate Models, Rep. 5*, edited by V. Eyring, T. G. Shepherd, and D. W. Waugh, pp. 379–412, World Meteorol. Organiz., Geneva, Switzerland.

Butchart, N., et al. (2010), Stratospheric dynamics, in *SPARC Report on the Evaluation of Chemistry-Climate Models*, edited by V. Eyring, T. G. Shepherd, and D. W. Waugh, pp. 109–148, World Meteorol. Organiz., Geneva, Switzerland.

Butchart, N., et al. (2011), Multimodel climate and variability of the stratosphere, *J. Geophys. Res.*, *116*, D05102, doi:10.1029/2010JD014995.

Calvo, N., R. R. Garcia, D. R. Marsh, M. J. Mills, D. E. Kinnison, and P. J. Young (2012), Reconciling modeled and observed temperature trends over Antarctica, *Geophys. Res. Lett.*, *39*, L16803, doi:10.1029/2012GL052526.

Charney, J. G., and P. G. Drazin (1961), Propagation of planetary scale disturbances from the lower into the upper atmosphere, *J. Geophys. Res.*, *66*, 83–109, doi:10.1029/JZ066i001p00083.

Cionni, I., V. Eyring, J. F. Lamarque, W. J. Randel, D. S. Stevenson, F. Wu, G. E. Bodeker, T. G. Shepherd, D. T. Shindell, and D. W. Waugh (2011), Ozone database in support of CMIP5 simulations: Results and corresponding radiative forcing, *Atmos. Phys. Chem.*, *11*, 11,267–11,292, doi:10.5194/acp-11-11267-2011.

Collins, W. D., et al. (2006), The Community Climate System Model version 3 (CCSM3), *J. Clim.*, *19*, 2122–2143, doi:10.1175/JCLI3761.1.

Dee, D. P., et al. (2011), The ERA-Interim reanalysis: Configuration and performance of the data assimilation system, *Q. J. R. Meteorol. Soc.*, *137*, 553–597, doi:10.1002/qj.828.

Donner, L. J., et al. (2011), The dynamical core, physical parameterizations, and basic simulation characteristics of the atmospheric component AM3 of the GFDL Global Coupled Model CM3, *J. Clim.*, *24*, 3484–3519.

Forster, P. M. D., and K. P. Shine (1997), Radiative forcing and temperature trends from stratospheric ozone changes, *J. Geophys. Res.*, *102*, 10,841–10,855, doi:10.1029/96JD03510.

Fu, Q., P. Lin, S. Solomon, and D. L. Hartmann (2015), Observational evidence of strengthening of the Brewer-Dobson circulation since 1980, *J. Geophys. Res. Atmos.*, *120*, 10,214–10,228, doi:10.1002/2015JD023657.

Garfinkel, C. I., D. W. Waugh, and L. M. Polvani (2015), Recent Hadley cell expansion: The role of internal atmospheric variability in reconciling modeled and observed trends, *Geophys. Res. Lett.*, *42*, 10,824–10,831, doi:10.1002/2015GL066942.

Gerber, E. P., and S.-W. Son (2014), Quantifying the summertime response of the austral jet stream and Hadley cell to stratospheric ozone and greenhouse gases, *J. Clim.*, *27*, 5538–5559, doi:10.1175/JCLI-D-13-00539.1.

Grise, K. M., L. M. Polvani, G. Tselioudis, Y. Wu, and M. D. Zelinka (2013), The ozone hold indirect effect: Cloud-radiative anomalies accompanying the poleward shift of the eddy-driven jet in the Southern Hemisphere, *Geophys. Res. Lett.*, *40*, 3688–3692, doi:10.1002/grl.50675.

Holton, J. R., P. H. Haynes, M. E. McIntyre, A. R. Douglass, R. B. Rood, and L. Pfister (1995), Stratosphere-troposphere exchange, *Rev. Geophys.*, *33*, 403–439, doi:10.1029/95RG02097.

Ivy, D. J., S. Solomon, and H. E. Rieder (2016), Radiative and dynamical influences on polar stratospheric temperature trends, *J. Clim.*, *29*, 4927–4938, doi:10.1175/JCLI-D-15-0503.1.
Johanson, C. M., and Q. Fu (2009), Hadley cell widening: Model simulations versus observations, *J. Clim.*, *22*, 2713–2725.
Kang, S., L. M. Polvani, J. C. Fyfe, and M. Sigmond (2011), Impact of polar ozone depletion on subtropical precipitation, *Science*, *332*, 951–954, doi:10.1126/science.1202131.
Kharin, V. V., and J. F. Scinocca (2012), The impact of model fidelity on seasonal predictive skill, *Geophys. Res. Lett.*, *36*, L22706, doi:10.1029/2009GL040367.
Kiehl, J. T., and B. A. Boville (1988), The radiatve-dynamical response of a stratospheric-tropospheric general circulation model to changes in ozone, *J. Atmos. Sci.*, *45*, 1798–1817.
Kiehl, J. T., B. A. Boville, and B. P. Briegleb (1988), Response of a general circulation model to a prescribed Antarctic ozone hole, *Nature*, *332*, 501–504.
Lee, S., and S. B. Feldstein (2013), Detecting ozone- and greenhouse gas-driven wind trends with observational data, *Science*, *339*, 563–567, doi:10.1026/science.1225154.
Li, F., J. Austin, and J. Wilson (2008), The strength of the Brewer-Dobson circulation in a changing climate: Coupled chemistry-climate model simulations, *J. Clim.*, *21*, 40–57, doi:10.1175/2007JCLI1663.1.
Lin, P., and Q. Fu (2013), Changes in various branches of the Brewer-Dobson circulation from an ensemble of chemistry climate models, *J. Geophys. Res. Atmos.*, *118*, 73–84, doi:10.1029/2012JD018813.
Mahlman, J. D., J. P. Pinto, and L. J. Umscheid (1994), Transport, radiative, and dynamical effects of the Antarctic ozone hole: A GFDL "SKYHI" model experiment, *J. Atmos. Sci.*, *51*, 489–508.
Manzini, E., B. Steil, C. Brühl, M. A. Giorgetta, and K. Krüger (2003), A new interactive chemistry-climate model: 2. Sensitivity of the middle atmosphere to ozone depletion and increase in greenhouse gases and implication for recent stratospheric cooling, *J. Geophys. Res.*, *108*(D14), 4429, doi:10.1029/2002JD002977.
McLandress, C., A. I. Jonsson, D. A. Plummer, M. C. Reader, J. F. Scinocca, and T. G. Shepherd (2010), Separating the dynamical effects of climate change and ozone depletion. Part I Southern Hemisphere stratosphere, *J. Clim.*, *23*, 5002–5020, doi:10.1175/2010JCLI3586.1.
McLandress, C., T. G. Shepherd, J. F. Scinocca, D. A. Plummer, M. Sigmond, A. I. Jonsson, and M. C. Reader (2011), Separating the dynamical effects of climate change and ozone depletion. Part II: Southern Hemisphere troposphere, *J. Clim.*, *24*, 1850–1868, doi:10.1175/2010JCLI3958.1.
Polvani, L. M., D. W. Waugh, G. J. P. Correa, and S. W. Son (2011), Stratospheric ozone depletion: The main driver of twentieth-century atmospheric circulation changes in the Southern Hemisphere, *J. Clim.*, *24*, 795–812, doi:10.1175/2010JCLI3772.1.
Polvani, L. M., L. Wang, V. Aquila, and D. W. Waugh (2017), The impact of ozone depleting substances on tropical upwelling, as revealed by the absence of lower stratospheric cooling since the late 1990s, *J. Clim.*, *30*, 2523–2534.
Ramaswamy, V., M. D. Schwarzkopf, and K. P. Shine (1992), Radiative forcing of climate from halocarbon-induced global stratospheric ozone loss, *Nature*, *355*, 810–812, doi:10.1038/355810a0.
Ramaswamy, V., et al. (2001), Stratospheric temperature trends: Observations and model simulations, *Rev. Geophys.*, *39*, 71–122, doi:10.1029/1999RG000065.
Ramasway, V., and M. M. Bowen (1994), Effect of changes in radiatively active species upon the lower stratospehric temperatures, *J. Geophys. Res.*, *99*, 18,909–18,921.
Randel, W. J., and F. Wu (1999), Cooling of the Arctic and Antarctic polar stratospheres due to ozone depletion, *J. Clim.*, *12*, 1467–1479.
Seviour, W. J. M., D. W. Waugh, L. M. Polvani, G. J. P. Correa, and C. I. Garfinkel (2017), Robustness of the simulated tropospheric response to ozone depletion, *J. Clim.*, *30*, 2577–2585, doi:10.1175/JCLI-D-16-0817.1.
Shine, K. P. (1987), The middle atmosphere in the absence of dynamical heat fluxes, *Q. J. R. Meteorol. Soc.*, *113*, 603–633, doi:10.1002/qj.49711347610.
Solomon, S. (1999), Stratospheric ozone depletion: A review of concepts and history, *Rev. Geophys.*, *37*, 275–316, doi:10.1029/1999RG900008.
Son, S.-W., et al. (2010), Impact of stratospheric ozone on Southern Hemisphere circulation change: A multimodel assessment, *J. Geophys. Res.*, *115*, D00M07, doi:10.1029/2010JD014271.
Sun, L., G. Chen, and W. A. Robinson (2014), The role of stratospheric polar vortex breakdown in Southern Hemisphere climate trends, *J. Atmos. Sci.*, *71*, 2335–2353, doi:10.1175/JAS-D-13-0290.1.
Thompson, D. W. J., and S. Solomon (2002), Interpretation of recent Southern Hemisphere climate change, *Science*, *296*, 895–899, doi:10.1126/science1069270.
Wang, L., and D. W. Waugh (2012), Chemistry-climate model simulations of recent trends in lower stratospheric temperature and stratospheric residual circulation, *J. Geophys. Res.*, *117*, D09109, doi:10.1029/2011JD017130.
Waugh, D. W., F. Primeau, T. DeVries, and M. Holzer (2013), Recent changes in ventilation of the Southern Oceans, *Science*, *339*, 568–570, doi:10.1126/science.1225411.
Waugh, D. W., C. I. Garfinkel, and L. M. Polvani (2015), Drivers of the recent tropical expansion in the Southern Hemisphere: Changing SSTs or ozone depletion, *J. Clim.*, *28*, 6581–6586, doi:10.1175/JCLI-D-15-0138.1.
Young, P. J., A. H. Butler, N. Calvo, L. Haimberger, P. J. Kushner, D. R. Marsh, W. J. Randel, and K. H. Rosenlof (2013), Agreement in late twentieth century Southern Hemisphere stratospheric temperature trends in observations and CCMVal-2, CMIP3 and CMIP5 models, *J. Geophys. Res. Atmos.*, *118*, 605–613, doi:10.1002/jgrd.50126.